Meloidogyne enterolobii MeMSP1 effector targets the glutathione-S -transferase phi GSTF family in Arabidopsis to manipulate host metabolism and promote nematode parasitism

Yongpan Chen, Qian Liu, Xuqian Sun, Lei Liu, Jianlong Zhao, Shanshan Yang, Xiangfeng Wang, Michaël Quentin, Pierre Abad, Bruno Favery, et al.

Meloidogyne enterolobii MeMSP1 effector targets the glutathione-S-transferase phi GSTF family in Arabidopsis to manipulate host metabolism and promote nematode parasitism

Yongpan Chen[1], Qian Liu[1,2], Xuqian Sun[1], Lei Liu[1], Jianlong Zhao[3], Shanshan Yang[4], Xiangfeng Wang[5], Michaël Quentin[6], Pierre Abad[6], Bruno Favery[6*], Heng Jian[1*]

[1] Department of Plant Pathology and MOA Key Laboratory of Pest Monitoring and Green Management, China Agricultural University, Beijing 100193, China; [2] Sanya Institute of China Agricultural University, Sanya 572024, China; [3] Institute of Vegetables and Flowers, Chinese Academy of Agricultural Science, Beijing, 100081, China; [4] College of Agriculture, Guangxi University, Nanning, 530004, Guangxi, China; [5] National Maize Improvement Center, College of Agronomy and Biotechnology, China Agricultural University, Beijing 100193, China; [6] INRAE, Université Côte d'Azur, CNRS, ISA, Sophia Antipolis F-06903, France

*** Authors for correspondence**

Prof. Heng Jian

Yuanmingyuan West Road No. 2, Haidian District, Beijing 100193, China

Tel: +86 135 5248 1996

Email: hengjian@cau.edu.cn

Dr. Bruno Favery

400 route des chappes, BP 167, 06900 Sophia Antipolis, France

Email: bruno.favery@inrae.fr

ORCID

Yongpan Chen 0000-0001-9074-7199, https://orcid.org/0000-0001-9074-7199

Qian Liu 0000-0001-6621-2266, https://orcid.org/0000-0001-6621-2266

Xuqian Sun 0000-0001-5387-7605, https://orcid.org/0000-0001-5387-7605

Jianlong Zhao 0000-0002-8179-6885, https://orcid.org/0000-0002-8179-6885

Shanshan Yang 0000-0002-2371-3981, https://orcid.org/0000-0002-2371-3981

Heng Jian 0000-0002-5908-3272, https://orcid.org/0000-0002-5908-3272

Pierre Abad 0000-0003-0062-3876, https://orcid.org/0000-0003-0062-3876

Bruno Favery 0000-0003-3323-1852, https://orcid.org/0000-0003-3323-1852

Michaël Quentin 0000-0002-8030-1203, https://orcid.org/0000-0002-8030-1203

Total word count (excluding summary, references and legends):	6233	Acknowledgements:	104
Summary:	188	Author contributions:	68
Introduction:	900	No. of figures:	8 (all Figs in colour)
Materials and Methods:	1986	No. of Tables:	1
Results:	1758	No of Supporting Information files:	25 (Fig S1-S16, Tables S1-S9)
Discussion:	1417		

Brief heading: Root-knot nematode secretes MeMSP1 effector to manipulate host metabolism and promote nematode parasitism

Twitter @brunofavery

Summary

- *Meloidogyne enterolobii* is an emerging root-knot nematode species that overcomes most of the nematode resistance genes in crops. Nematode effector proteins secreted in planta are key elements in the molecular dialogue of parasitism. Here, we show the MeMSP1 effector is secreted into giant cells and promotes *M. enterolobii* parasitism.
- Using Co-IP and BiFC assays we identified glutathione-S-transferase phi GSTFs as host targets of the MeMSP1 effector. This protein family plays important roles in plant responses to abiotic and biotic stresses. We demonstrate that MeMSP1 interacts with all *Arabidopsis* GSTF. Moreover, we confirmed that the N-terminal region of AtGSTF9 is critical for its interaction, and *atgstf9* mutant lines are more susceptible to RKN infection.
- Combined transcriptome and metabolome analyses showed that MeMSP1 affects the metabolic pathways of *Arabidopsis thaliana*, resulting in the accumulation of amino acids, nucleic acids, and their metabolites, and organic acids and the down-regulation of flavonoids.
- Our study has shed light on a novel effector mechanism that targets plant metabolism, reducing the production of plant-defence related compounds while favouring the accumulation of metabolites beneficial to the nematode, and thereby promoting parasitism.

Keywords: *Arabidopsis thaliana*, Effector, Glutathione-S-transferase, *Meloidogyne enterolobii*, Pathogen, Plant metabolism, Root-knot nematode.

Introduction

Plant parasitic nematodes (PPNs) are one of the most economically important plant pathogens, causing more than 100 billion dollars loss annually worldwide (Abad *et al.*, 2008). Root-knot nematodes (RKNs; *Meloidogyne* spp.) are one of the greatest threats to agriculture production. RKNs infect more than 5,500 plant species and cause a global yield loss of 70 billion dollars every year (Blok *et al.*, 2008; Caboni *et al.*, 2012; Chen, J *et al.*, 2017). RKNs are sedentary endoparasitic nematodes that induce the formation of complex feeding cells in the vascular cylinder of host root, known as giant cells, which serve as the sole nutrient source for the development and reproduction of RKNs (Favery *et al.*, 2016; Rutter *et al.*, 2022). In order to establish parasitism successfully, RKNs need to suppress plant defence, induce and maintain the giant cells. They have evolved numerous secreted effectors that originate from the three oesophageal glands or other organs like amphids and hypodermis (Favery *et al.*, 2020; Zhao et al., 2019; Haegeman *et al.*, 2012). Although some effectors have predicted functions, e.g. redox-regulated proteins such as thioredoxins, glutathione peroxidases, glutathione-S-transferases (GST) and protein disulphide isomerases (PDI) (Bellafiore et al., 2008; Tian et al., 2019, Zhao et al 2021), a large majority of these effectors are pioneers without known functional domains (Jagdale *et al*., 2021; Goverse & Mitchum, 2022). The identification of host targets of these RKN pioneer effectors is one of the strategies to understand their roles in the parasitism.

Only a few plant targets of RKN effectors have been identified (reviewed by Mejias *et al.*, 2019 and Rutter *et al.,* 2022) and recently several targets involved in defence or stress response have been characterised. A stress-associated protein from *Solanaceae* and *Arabidopsis* has been shown to be targeted by *M. incognita* MiPDI1 to establish disease (Zhao *et al.*, 2020). The C-type lectin effector MiCTL1a interacts with plant catalases to regulate the redox state in the host (Zhao *et al.*, 2021). Another example is the *M. graminicola* MgMO289 effector that interacts with the rice heavy metal-associated plant protein 04 (OsHPP04) to modulate host superoxide dismutase (SOD) activity and scavenge reactive oxygen species (Song et al., 2021). In addition, the *M. enterolobii* translationally controlled tumour protein (MeTCTP) is able to

homodimerise to bind calcium and prevent cytosolic calcium rise in order to suppress plant immunity (Guo et al., 2022). However, the targets and functions of RKN effectors are still largely unknown.

Plant metabolism play a central role in the molecular dialogue during plant-pathogen interactions. Giant cells are a metabolic sink that act as the nutrient source for the developing nematode. During giant cell formation, RKNs modified physiological and transport processes of host cells, resulting in altered metabolite production and transport (Bartlem *et al.*, 2014). Studying the changes in host plant metabolites caused by nematodes allows a better understanding of the giant cell. An untargeted proton Nuclear Magnetic Resonance (1H-NMR) analysis of primary metabolites in roots and galls 21 days post infection (dpi) with *M. incognita* of normal and (homo) glutathione (h)GSH depleted *Medicago truncatula* identified 15 metabolites (sugars, organic acids, and amino acids) significantly different between galls and uninfected roots (Baldacci-Cresp et al, 2012). This study showed that (h)GSH depletion affects gall metabolism (Baldacci-Cresp *et al.*, 2012). The metabolite concentration is higher in galls than in roots at 35 dpi resulting in water potential and osmotic pressure modification in galls (Baldacci-Cresp *et al.*, 2015). Gas chromatography coupled to mass spectrometry untargeted fingerprint analysis was also used to analyse metabolites in tomato leaves and stem upon *M. incognita* infection (Eloh *et al.*, 2016). However, the effects of RKN effectors on host metabolism is limited.

Meloidogyne enterolobii (syn. *M. mayaguensis*) is one emergent species, first reported in 1983, that can overcome RKN resistance genes such as the *Mi-1.2* gene (tomatoes), *Mh* gene (potato), *Mir1* gene (soybean), *N* gene (bell pepper), *Tabasco* gene (sweet pepper) and *Rk* gene (cowpea) (Yang & Eisenback, 1983; Castagnone-Sereno, 2012; Philbrick *et al.*, 2020). Utilizing RNA interference (RNAi) to silence *M. enterolobii* specific effector genes or the effector targets may be an opportunity to enhance plant resistance to this uncontrolled RKN. MeTCTP silencing resulted in reduced parasitism of *M. enterolobii* on tomato (Zhuo *et al.*, 2017). The EFFECTOR18 (EFF18) protein is a conserved RKN effector, and both *M. incognita* and *M. enterolobii* EFF18 have been shown to interact with the spliceosomal small nuclear ribonucleoprotein D1 (SmD1)

from *A. thaliana*, *S. lycopersicum*, and *N. benthamiana* (Mejias *et al.*, 2021; Mejias *et al.*, 2022). Virus-induced gene silencing of *SmD1* in tomato affected giant cell formation and nematode development (Mejias *et al.*, 2022). Thus, this evidence shows that modifying the expression of RKN effectors or their target genes to improve plant resistance to *M. enterolobii* a promising approach.

In this study, we characterised a novel nematode effector mechanism in *M. enterolobii.* *M. incognita* MiMSP1 has been reported as a potential effector, as it is expressed in the dorsal gland of parasitic RKNs, although there are no further reports on its functional analysis (Huang *et al.*, 2003). We demonstrated that its ortholog MeMSP1 is secreted into the host through the stylet, is capable of physically interacting with all *Arabidopsis* glutathione-S-transferase phi proteins (AtGSTF), and found that the knockout (ko) mutant lines of *AtGSTF9* were more susceptible to RKN infection. Combined transcriptome and metabolome analyses revealed that ectopic expression of MeMSP1 in *Arabidopsis* affected host metabolic pathways and secondary metabolite biosynthesis.

Materials and Methods

Nematode and Plant materials and growth conditions

M. enterolobii were propagated on the susceptible tomato cultivar (*Solanum lycopersicum* L. cv. "Baiguo Qiangfeng") in a greenhouse starting from a single egg mass. Egg masses were collected and hatched according to Niu *et al* (Niu *et al.*, 2016). All seeds of *A. thaliana* (L.) Heynh were surface-sterilized and then grown on solidified half-strength Murashige and Skoog (MS) medium with 2% sucrose. The T-DNA insertion mutant lines of *AtGSTF9* (SALK_001519C and SALK_148672C) were obtained from the *Arabidopsi*s Biological Resource Center (ABRC, USA). *Nicotiana benthamiana* plants were grown in pots under long-day conditions (16h light/8 h dark) at 25^{o}C.

Sequence analysis, alignment and phylogenetic tree

MSP1 sequences were obtained from WormBase Parasite (https://parasite.wormbase.org/index.html) and *Meloidogyne* genomic resources

(http://www6.inra.fr/meloidogyne_incognita/) by blastp against the *Meloidogyne* predicted protein database, the protein sequences with a higher identity than 85.5% were selected. Multiple amino acid sequence alignment analyses of MSP1 proteins were conducted using DNAMAN V6 (Lynnon Biosof, USA). These MSP1 protein sequences were aligned with the MAFFT tool on the EBI server (https://www.ebi.ac.uk/Tools/msa/mafft/). The alignment was then used as input for the IQTree Web server (http://iqtree.cibiv.univie.ac.at/) to generate the maximum likelihood phylogenetic tree. The model chosen by the inbuilt model test was Flu+I. Support for the nodes was calculated with 100 bootstrap replicates. MiMSP12 was used as the outgroup in the phylogenetic tree for MeMSP1 putative orthologs. The tree was visualized in iTOL (https://itol.embl.de/).

RNA isolation and gene amplification

The mRNA of *M. enterolobii* was extracted using an RNAprep pure Micro Kit (Tiangen Biotech Co., Ltd Beijing), and total RNA of *Arabidopsis* was isolated from seedlings using TRIzol Reagent (Invitrogen, USA). Complementary DNA (cDNA) was synthesized using M-MLV reverse transcriptase (TaKaRa, Japan). *MeMSP1* genes were amplified from cDNA of *M. enterolobii* by PCR using specific primers (Table S1). The PCR products were cloned into pMD18-T vector (TaKaRa, Japan) and sequenced. All primers used in this study are listed in Supplementary Table S1 and were synthesized by TsingKe Biotechnology Co. Ltd, Beijing, China.

Developmental expression analysis and *in situ* hybridisation

mRNA samples of *M. enterolobii* at different life stages were obtained as above. The cDNA was synthesized using M-MLV reverse transcriptase (TaKaRa, Japan). qRT-PCR was conducted using the SYBR Premix Ex Taq II (Tli RNaseH Plus) (Takara, Japan). *GAPDH* gene of *M. enterolobii* was used as a control. The results were determined using the $2^{-\Delta\Delta CT}$ method. Three technical replicates for each reaction were performed in all experiments, and three independent experiments were conducted.

For *in situ* hybridisation, freshly hatched *M. enterolobii* pre-J2s were collected on a 0.5

μm sieve. The primers ISH-MeMSP1-F and ISH-MeMSP1-R were used to amplify the 179 - 491 bp (313 bp) of the MeMSP1 coding sequences (CDS) from cDNA, and the DIG-labelled sense (negative control) and antisense probes were synthesised by asymmetric PCR. The hybridisation were performed as described previously (Niu *et al.*, 2016) and examined using a BX51 microscope (Olympus, Japan).

Anti-MeMSP1 antibodies production and immunolocalisation analysis

The CDS of MeMSP1 without signal peptide was inserted into the pET-28a (+) vector and expressed in BL21 (DE3) cells. The purified recombinant MeMSP1 protein was used to produce polyclonal antibodies in rabbits at ABclonal Company (Wuhan, China). For immunolocalisation, galls of tomato (*Solanum lycopersicum* var. 'Baiguo') were harvested at 14 dpi, and were then fixed, dehydrated, embedded and sectioned as previously described (Vieira *et al.*, 2011). Anti-MeMSP1 antibodies and Goat anti-Rabbit Alexa Fluor 488 conjugated antibodies (Thermo Fisher Scientific, San Jose, CA, USA) were diluted 100- and 500-fold in blocking solution of 1% BSA in 50 mM piperazine-N, N'-bis (ethanesulphonic acid) (PIPES) buffer (pH 6.9), respectively. Nuclei were stained with 4', 6-diamidino-2-phenylindole (DAPI, 1μg/mL in water). Finally, slides were mounted with ProLong anti fade medium (Invitrogen, USA) and observed under confocal microscope at an excitation wavelength of 488 nm (Leica SP8, Germany).

Protein extraction and western blot analysis.

Total proteins of *N. benthamiana* leaves or *A. thaliana* seedlings were extracted using a protein extraction kit (CW0885, Beijing ComWin Biotech Co., Ltd., China). For western blot, total protein samples were separated on a 10% polyacrylamide gel and transferred onto a polyvinylidene difluoride (PVDF) membrane using a semi-dry transfer system (BioRad, USA). After blocked in 5% skimmed milk (in PBS, pH 7.2) for 1 hour, the membrane was incubated with horseradish peroxidase (HRP) tag-conjugated antibodies (anti-Flag or anti-HA, MBL, China) diluted (1 : 5000) with PBS (pH 7.2) containing 1% skimmed milk for 1 hour. After washes, the membrane was

detected using an EasySee Western Blot Kit (DW101, TransGen Biotech, China) and imaged with a multifunctional molecular imaging system through automatic exposure (C600, AZURE).

Generation of transgenic *Arabidopsis* and infection assays

For *in planta* RNAi, a specific fragment (300 bp) of MeMSP1 was amplified and then inserted into a pSAT5 RNAi plasmid (Dafny-Yelin *et al.*, 2007). For ectopic expression of MeMSP1 in *Arabidopsis*, the ORF without signal peptide of MeMSP1 was cloned and inserted into Super1300-FLAG. These constructs were transformed into *Agrobacterium tumefaciens* GV3101 and used for transformation of *A. thaliana* via the floral dip method (Clough & Bent, 1998). Homozygous single insertion T3 plants were used for the susceptibility experiment to nematode. The plants were grown in pots (length: 5.5cm, width: 5.5cm, and height: 5cm) with soil (nutrient soil, Fangjie Company, China) and vermiculite (1: 1) under a growth chamber condition (22°C, 16 h: 8 h, light: dark photoperiod). Three-week-old *Arabidopsis* were inoculated with 300 freshly hatched J2s per plant. 14 days after infection, roots from MeMSP1-Ri lines and WT plants were collected and digested in a mixture of pectinase (P2611, Sigma) and cellulose (C2730, Sigma) at 28 °C and 160 rpm overnight. Parasitic nematodes were collected under a stereomicroscope and used to measure the expression level of *MeMSP1* by qRT-PCR. Roots were collected 30 days after infection and stained using the sodium hypochlorite-acid fuchsin method (Bybd *et al*., 1983). The numbers of galls, females and other stage nematodes were counted under a stereomicroscope microscope (SZ61, Olympus, Tokyo, Japan). At least 15 plants of each transgenic line or wild-type (Col-0; WT) were used for each experiment and three independent experiments were performed.

Interaction analysis

For identifying the target of MeMSP1 in *Arabidopsis*, total proteins were extracted from MeMSP1-expressing lines (MeMSP1-OE-1 and MeMSP1-OE-3) and WT plants. Immunoprecipitation (IP) was performed using anti-FLAG M2 affinity gel resin

(Sigma-Aldrich, USA). Proteins were eluted with competitive 3X FLAG peptide (F4799, Sigma-Aldrich, USA). Q Exactive (Thermo Q-Exactive nanospray ESI-MS mass spectrometer, USA) was used for liquid chromatography-tandem mass spectrometry (LC-MS/MS) at China Agricultural University Functional Genomics Platform. The acquired MS data were pre-analysed using Mascot Distiller 2.4 (UK) and then anatomized to search a NCBI non-redundant protein database and Swiss-prot database.

For bimolecular fluorescence complementation (BiFC) analysis, coding sequences (CDS) of *MeMSP1* without its signal peptide and *AtGSTFs* were cloned into the pUC_SPYCE or the pUC_SPYNE vector (Walter *et al.*, 2004), respectively. AtGSTU19 (AT1G78380) and empty vectors were used as negative control. Mixtures of *A. tumefaciens* cells (OD600=0.5, respectively) containing each pair were co-infiltrated into the leaves of *N. benthamiana* and observed using a laser confocal fluorescence microscope (Leica SP8, Germany).

For co-immunoprecipitation (Co-IP) assays, the *AtGSTF* CDS were cloned into pGR107_flag vector and *MeMSP1* CDS without signal peptide was cloned into pGR107_HA. EGFP was cloned into pGR107_Flag as a negative control. All constructs were sequenced and introduced into *A. tumefaciens* GV3101. Co-infiltrations and immunoprecipitation were conducted as previously described (Zhao *et al.*, 2019).

Transcriptome Analysis of transgenic *Arabidopsi*s lines

Total RNA of MeMSP1-OE and WT lines were extracted from the 14 days *Arabidopsis* seedlings with Spin Column Plant total RNA Purification Kit following the manufacturer's protocol (Sangon Biotech, Shanghai, China). The cDNA libraries were carried out as previously described (Chen, C *et al.*, 2017) and sequenced on the Illumina HiSeq platform (Illumina Inc., San Diego, USA) by Wuhan MetWare Biotechnology Co., Ltd. (www.metware.cn, Wuhan, China). The sequenced reads were compared with the unigene library using Bowtie (Langmead *et al.*, 2009), and the expression level was estimated in combination with RSEM (Li & Dewey, 2011). The gene expression level

was determined according to the FPKM. DESeq2 package (Love *et al.*, 2014; Varet *et al.*, 2016) was used to identify the differentially expressed genes (DEGs) between WT and MeMSP1-OE, with the |log2Fold Change| >= 1 and FDR (False Discovery Rate) < 0.05. KOBAS2.0 was used for the KEGG pathway enrichment analysis of the DEGs (Xie *et al.*, 2011). Two biological repeats were used for the Col-0 line and three biological repeats were used for the MeMSP1-OE-1 and MeMSP1-OE-3 lines in this transcriptome analysis， respectively. The DEGs shared by MeMSP1-OE-1 and MeMSP1-OE-3 *Arabidopsis* lines were analysed with NEMATIC, AgriGO (version 2, http://systemsbiology.cau.edu.cn/agriGOv2/) and compared with previous RNAseq data (Cabrera *et al.*, 2014; Tian *et al.*, 2017; Yamaguchi *et al.*, 2017).

Metabolome Analysis of transgenic *Arabidopsis* lines

Three biological repeats for transgenic lines (MeMSP1-OE-1 and MeMSP1-OE-3) and Col-0 were used for metabolome analysis. The samples were extracted from frozen 14-days-old seedlings overnight at 4°C with 70% aqueous methanol. All procedures related to metabolomics analysis were performed at Wuhan MetWare Biotechnology Co., Ltd. (www.metware.cn) following their standard procedures (Zhang *et al.*, 2019). The data acquisition instrument system included Ultra Performance Liquid Chromatography (UPLC) (Shim-pack UFLC SHIMADZU CBM30A, Tokyo, Japan) and tandem mass spectrometry (MS/MS) (Applied Biosystems 6500 QTRAP). Based on the self-built database MWDB (Metware database), the metabolites were characterized according to the secondary spectrum information. Metabolite quantification was performed using multiple reaction monitoring (MRM) in triple quadrupole mass spectrometry (Fraga *et al.*, 2010).

Data matrices with the intensity of metabolite feature under-treated and control conditions were uploaded to the Analyst 1.6.1 software (AB SCIEX, Ontario, Canada). For statistical analysis, missing values were assumed to be below the limits of detection, and these values were imputed with a minimum compound value (Chen *et al.*, 2013). Orthogonal partial least squares-discriminant analysis (OPLS-DA) was used to maximize the metabolome difference between the control and treated samples. The

relative importance of each metabolite to the OPLS-DA model was checked using a parameter variable importance in projection (VIP). Metabolites with fold change≥2 or fold change ≤0.5 and VIP ≥1 were considered as differential metabolites for group discrimination. KEGG pathway analysis was performed in the R software (www.r-project.org).

Bio-assay of the lethal effect of metabolites on *M. enterolobii* J2s

All tested compounds were purchased from Alphabio life science company (www.51alphabio.com). Compounds were dissolved in dimethyl sulfoxide to prepare a stock solution of 50 mg/ml. Four concentrations (10, 25, 50, 100 μg/ml) for butin and three concentrations for naringenin (10, 25, 50 μg/ml; due to the low solubility in water, naringenin recrystallized in the tested solution when we increased the concentration to 100 μg/ml) were tested for the nematode lethal effect assay. Controls (CK) consisted of the corresponding concentration of DMSO in water. Around 100 freshly hatched second-stage juveniles (J2s) were used for each repetitions. The dead nematode was counted every 24 h for 3 days (24 h, 48 h, and 72 h) under stereomicroscope microscope (SZ61, Olympus, Japan). All this experiment were done in 24-well plate, and the total volume is 1 ml each well. For each metabolites 3 independent experiments were performed, with six replicates for each treatment in each experiment.

Statistical analysis

The data were analysed with Dunnett's multiple comparisons test of one-way ANOVA. Statistical computations were carried out with GraphPad Prism (GraphPad Software Inc., La Jolla, CA, USA).

Accession numbers

Sequence data from this article can be found in the *Arabidopsis* Information Resource (https://www.arabidopsis.org), WormBase Parasite and GenBank/EMBL databases under the following accession numbers: MeMSP1 (OQ256232), *MiMSP12 (AY134431)*, *AtGSTF2* (*At4g02520*), *AtGSTF3* (*At2g02930*), *AtGSTF4* (*At1g02950*), *AtGSTF5*

(*At1g02940*), *AtGSTF6* (*At1g0293*), *AtGSTF7* (*At1g02920*), *AtGSTF8* (*At2g47730*), *AtGSTF9* (*At2g30860*), *AtGSTF10* (*At2g30870*), *AtGSTF11* (*At3g03190*), *AtGSTF12* (*At5g17220*), *AtGSTF13* (*At3g62760*), *AtGSTF14* (*At1g49860*), *MjMSP1 (M.Javanica_Scaff11723g062660)*, *MiMSP1 (Minc3s00173g06738)*, *MaMSP1a (M.Arenaria_Scaff41g001480)*, *MaMSP1b (M.Arenaria_Scaff1390g022660)* and *MfMSP1 (M.fscf7180000424015.g12030)*. The transcriptome data are available at the Sequence Read Archive (SRA) via accession number PRJNA933796. The metabolomic data are available at MetaboLights via accession number MTBLS7145.

RESULTS

MeMSP1 is highly upregulated during *M. enterolobii* parasitism

A homolog of *M. incognita* dorsal oesophageal gland cell secretory protein 1 (*MiMSP1*) was identified in the *M. enterolobii* transcriptome (*isotig 10924*) and was designated *MeMSP1* (Li *et al.*, 2016). The *MeMSP1* gene contains an open reading frame (ORF) of 525 bp that encodes a 174-amino-acid (aa) polypeptide that had no known functional domain except a secretion signal peptide of 20 amino acids at its N-terminus according to SignalP 5.0. This indicates MeMSP1 may be secreted from gland cells. According to previous report, there is a Mel-DOG box (TGCACTT) motif in the 346 bp upstream of the CDS of *MeMSP1* (Fig. S1) suggesting it may be specifically expressed in the dorsal gland of RKNs (da Rocha *et al.*, 2021). Five MSP1 homologues were obtained from the genome sequences of *Meloidogyne* spp. by blast against all protein databases. The MeMSP1 protein shared approximatively 85.7% aa sequence identity with the other *Meloidogyne* species homologs (Fig. 1a). The alignment and a maximum likelihood phylogenetic tree showed with six MSP1 protein sequences from *M. enterolobii*, *M. incognita*, *M. arenaria*, *M. floridensis* and *M. javanica* grouped together (Fig. 1b).

The developmental expression level of the *MeMSP1* gene in different stages of *M. enterolobii* was analysed by quantitative real-time PCR (qRT-PCR). Using the expression level of *MeMSP1* at the egg stage as a reference for calculating the relative fold changes in the other stages, *MeMSP1* was more strongly expressed in the parasitic

juveniles and females from 10 to 30 dpi, with a maximum at 10 dpi (Fig. S2a). Interestingly, the RNAseq data of *M. incognita* showed *MiMSP1* upregulated in parasitic stage (Fig. S2b) (Rocha *et al.*, 2021), we hypothesise the *MeMSP1* is also upregulated in the parasitic stage. These results indicate that *MeMSP1* is highly upregulated during giant cell formation *in planta*.

MeMSP1 is expressed in the dorsal gland and secreted into the nematode feeding site

In situ hybridisation was used to investigate the tissue localisation of *MeMSP1* in *M. enterolobii* J2s. Signals were observed in the dorsal gland cell of J2s (n=14) after hybridisation with the digoxigenin-labelled antisense probe (Fig. 2a). No signal was observed when using the sense probe as a negative control (Fig. 2b). A polyclonal antibodies was raised against MeMSP1 to analyse the localisation of MeMSP1 in the nematode and plant tissue. Western blot showed a clear hybridising band in the total protein samples from *M. enterolobii* J2s and in the recombinant MeMSP1 extract. No band was observed in the protein sample from healthy tomato roots (Fig. S3a), nor with the pre-immune serum in all the three protein samples (Fig. S3b). These results illustrated that the anti-MeMSP1 polyclonal antibodies can specifically recognize MeMSP1. Immunolocalisations performed on parasitic juveniles of *M. enterolobii* showed signals in the dorsal gland cell and in the oesophagus (Fig. 2c-d, Fig. S4). No signal was observed when the pre-immune serum was used as a negative control (Fig. 2e). To determine whether MeMSP1 is actually secreted into host plants, immunolocalisation was performed on sections of tomato galls collected 14 dpi. Signals were consistently observed in the cytoplasm of giant cells (Fig. 2f-h, Fig. S5). No signal was observed in the gall sections incubated with pre-immune serum (Fig. 2i). These results demonstrated that MeMSP1 is produced in the dorsal gland and secreted into the feeding cells in the host plant roots.

***MeMSP1* is involved in nematode parasitism**

In planta RNA silencing was used to investigate the role of *MeMSP1* gene in the

parasitism of *M. enterolobii*. The RNAi construct targeting *MeMSP1* was developed and transferred into *Arabidopsis*, and three homozygous MeMSP1-RNAi lines (MeMSP1-Ri) were used for RKN infection assays. One homozygous RNAi transgenic *Arabidopsi*s line targeting GFP (GFP-Ri) and the wild-type Col *Arabidopsis* were used as controls. At 14 dpi, nematodes from all tested *Arabidopsis* lines were extracted to measure the *MeMSP1* transcript abundance. We found a strong reduction of the transcript level of *MeMSP1* in the nematodes recovered from MeMSP1-Ri lines (Fig. 3a). Infection assays showed that the numbers of galls, parasitic juveniles and nematode females were significantly decreased in MeMSP1-Ri lines, compared to the controls at 30 dpi (Fig. 3b; Fig. S6).

Moreover, two independent homozygous transgenic *Arabidopsis* lines expressing *MeMSP1* (MeMSP1-OE) were generated (Fig. S7). Infection assays showed these transgenic lines were both significantly ($P < 0.05$) more susceptible to *M. enterolobii* infection, with 30% more galls and parasitic nematodes at 30 dpi than the controls (COL and plants transformed with an empty super1300 vector) (Fig. 3c; Fig. S6). These results demonstrated that MeMSP1 play important roles in *M. enterolobii* parasitism.

MeMSP1 interacts with all the GSTF family members of *Arabidopsis*

To identify the plant targets of MeMSP1, we performed *in planta* immunoprecipitation (IP) followed by liquid chromatography-tandem mass spectrometry (LC-MS) on MeMSP1-OE-1, MeMSP1-OE-3 plants and WT *Arabidops*is. Among the candidate proteins that were pulled down in both MeMSP1-OE plants (Table S2), but not in WT plants, three *Arabidopsis* glutathione-S-transferase phi (AtGSTF2, AtGSTF9 and AtGSTF10) proteins were identified that are localised in the cytosol as MeMSP1 (Fig. S8) (Dixon *et al.*, 2009). The AtGSTFs is a large plant-specific class of proteins with 13 members in *Arabidopsis*. Only a few members appear differentially expressed in the galls, either overexpressed and/or repressed (Table S3). We then investigated the interactions between MeMSP1 and the 13 AtGSTFs (AtGSTF2 to AtGSTF14) using BiFC and Co-IP assays.

For Co-IP, the Flag-AtGSTFs and MeMSP1-HA expression constructs were co-

expressed in *N. benthamiana* leaves. Flag-eGFP was used as a negative control. All the proteins were correctly expressed in tobacco leaves as evidenced by their detection with anti-Flag and anti-HA antibodies (Fig. 4a). Analysis of the immunoprecipitated protein samples with anti-HA antibodies showed that under the same conditions, MeMSP1-HA was specifically pulled down by Flag-AtGSTFs, but not by Flag-eGFP (Fig. 4a). Furthermore, BiFC assays in *N. benthamiana* leave cells showed that the YFP fluorescence signals were observed in the cytoplasm of *N. benthamiana* epidermal cells that co-expressed the MeMSP1-YFPn fusion and each of the 13 AtGSTF-YFPc construct (Fig. 4b, Fig. S9), but not with the controls. These results demonstrated that MeMSP1 specifically interacts *in planta* with the AtGSTF family members.

AtGSTF9 is involved in plant immunity to nematodes

MS data showed that AtGSTF9 had the highest score of all identified GSTF proteins (Table S2). Moreover, AtGSTF9 has been shown to be involved in plant immunity (Horváth *et al.*, 2015; Gong *et al.*, 2018). We therefore focused on this gene for further analysis of its interaction with MeMSP1 and function in nematode parasitism. Typical of AtGSTFs, the AtGSTF9 protein contains a conserved N-terminal thioredoxin-fold domain (1-75 aa) for the conjugation of reduced glutathione and a C-terminal alpha-helical domain (90-208 aa) for the conjugation of hydrophobic substrate. To investigate which domain is important to the interaction, three mutant structures of AtGSTF9 were constructed, AtGSTF9-N-mu, AtGSTF9-C-mu and AtGSTF9-NC-mu (Fig. S10). BiFC assays showed fluorescence only in the positive control and in the leaves infiltrated with AtGSTF9-C-mu-YFPc construct (Fig. 5a). These results showed that the N-terminal part of AtGSTF9 is essential for the interaction between MeMSP1 and AtGSTF9.

To investigate the role of AtGSTF9 in plant response to RKN, we obtained two T-DNA insertional alleles of *AtGSTF9* (Salk_001519C, Salk148672C). No *AtGSTF9* transcripts were detected in plants homozygous for the insertions (Fig. S11). These *gstf9* ko lines were significantly more susceptible to *M. enterolobii* than control plants, illustrated by a higher number of galls and nematodes inside roots (Fig. 5b; Fig. S12). This result

showed that AtGSTF9 has a role in plant immunity to *M. enterolobii*.

Expression of *MeMSP1* affects metabolic pathways and the biosynthesis of secondary metabolites in *Arabidopsis*

To understand the mode of action of MeMSP1, we investigated genes and metabolites differentially expressed/accumulated in MeMSP1-OE lines compared to WT seedlings, by combining transcriptomic and metabolomic analyses. Transcriptome data identified 696 differentially expressed genes (DEG) in both MeMSP1-OE- lines compared to WT. 288 DEGs are downregulated and 407 upregulated (Fig. 6a, b; Table S4-S6). Eight DEGs (four upregulated and four down-regulated) were selected to validate the transcriptome data through qPCR, and the results of three biological replicates were consistent with the transcriptome results (Fig. S13). Among these downregulated DEGs, we identified *AtGSTF3* (*At2g02930*), one of the targets of MeMSP1, *TPI* (*At1g73260*), a gene downregulated in galls that have been validated by qRT-PCR (Jammes *et al.*, 2005). Interestingly *CCS52B* (*At5g13840*), strongly induced in galls (de Almeida *et al.*, 2012), was identified in the upregulated DEGs. The KEGG analysis of shared DEGs revealed that the "metabolic pathways" and "biosynthesis of secondary metabolites" were the two most significantly enriched pathways in the two MeMSP1-OE lines (Fig. 6c). Gene ontology (GO) analysis of the common DEGs showed enrichment in the GO terms "oxidation-reduction process" and "oxidoreductase activity", indicating that *MeMSP1* expression affects the oxidation-reduction balance in *Arabidopsis* (Fig. S14). Metabolome data identified differently accumulated metabolites (DAMs), 13 with a lower content and 25 with a higher content, in both MeMSP1-OE lines (Fig. 7a, b, Table S7 to S9). Among these, amino acid derivatives, nucleic acids and their metabolites, and organic acids all showed upregulated accumulation, while most flavonoids like flavanone, flavone, and flavonolignan showed downregulated accumulation (Table 1). Three metabolites, GSH, L-CYS-GLY, and γ-Glu-Cys involved in the glutathione cycle were significantly accumulated (Table 1). Most DAMs are involved in metabolic pathways by KEGG classification analysis (Fig. 7c). These combined analyses demonstrated that MeMSP1 modulates the metabolic pathway and biosynthesis of

secondary metabolite pathways in *Arabidopsi*s.

Down-regulated metabolites show a harmful effect on nematodes

Of the 13 DAMs with lower levels, 11 belong to the flavonoid family, a well-known group of plant defence compounds. To investigate their roles against RKN, we first tested the mortality of five compounds at 50 mg/L by soaking *M. enterolobii* J2s for 48 hours. Three of these had significant and reproducible paralysis activity, namely naringenin, N', N''-di-p-coumaroyl spermidine and butin (Fig. S15). Different concentrations of butin and naringenin and different treatment times were tested on nematodes. The results showed that no significant effect on nematodes was observed when the 10 μg/ml concentration of butin and naringenin was used to treat nematodes for 24 h. With the increase in treatment time and the substances concentration, both butin and naringenin showed a lethal effect on nematodes compared with the control. And when nematodes were soaked with 50 μg/ml concentration for 72 hours, the mortality rate of butin and naringenin to nematodes reached 24.7% and 21.4% respectively. (Fig. 8; Fig. S16). This finding indicated that the expression of MeMSP1 in *A. thaliana* results in reduced accumulation of compounds that are harmful to nematodes.

Discussion

Meloidogyne spp. are obligate plant parasites with a worldwide distribution; they are considered the most devastating of plant-parasitic nematodes (Jones *et al.*, 2013). *M. enterolobii* is an emerging RKN species capable of overcoming most of the nematode resistance genes in crops (Sikandar *et al.*, 2022). One of the specific features of RKN interactions with plants is their ability to reprogram root cells to form specialised giant, hypertrophied, multinucleate feeding cells, which serve as their sole source of nutrients (Favery *et al*., 2020). RKN parasitism is facilitated by the secretion of a large number of effector proteins. The RKN effectors described to date have three major functions: (1) the degradation and modification of plant cell walls; (2) the suppression of host defences; (3) modulation of the physiology of the host plant to allow the formation and

the functioning of the permanent feeding site (Mitchum *et al.*, 2013). Here we identified a RKN effector that manipulate plant metabolism.

MeMSP1 is a conserved RKN-specific effector secreted into giant cells to promote parasitism

MeMSP1 orthologs have been found in five of the eight RKNs for which genome sequences are available (*M. incognita*, *M. javanica*, *M. arenaria*, *M. enterolobii* and *M. floridensis*). No such orthologs have been found in cyst nematodes and free-living nematodes (Li *et al.*, 2016). We performed immunolocalisation experiments, which confirmed the biosynthesis of MeMSP1 in the dorsal oesophageal gland of parasitic juveniles and the secretion of this molecule *in planta*. The host-induced gene silencing (HIGS) of *MeMSP1* in nematodes feeding on transgenic plants producing dsRNA and the overexpression *in planta* of the *MeMSP1* gene confirmed the role of this molecule as an effector involved in parasitism. The immunolocalisation of MeMSP1 in giant cells and the results of the HIGS experiments suggest that MeMSP1 acts during later stages of parasitism, after the nematode has become sedentary.

MeMSP1 interacts with glutathione-S-transferase phi GSTF proteins

Using biochemical and cell biology approaches, we were able to identify and validate the GST phi (GSTF) class of proteins as targets of MeMSP1 within the plant. Indeed, we found that MeMSP1 interacted with the 13 *Arabidopsis* GSTF proteins. GSTF proteins constitute a large plant-specific class of GSTs proteins. GSTs display significant sequence divergence, but crystallographic and biophysical studies have shown that their protein structure is conserved with a G-site at the N-terminus that specifically binds to GSH and an H-site that binds to the electrophilic substrate (Oakley, 2011). We found that several amino acids at the N-terminus of AtGSTF9 were essential for its interaction with MeMSP1, suggesting that MeMSP1 targets the G site, which is critical for GSTF function.

Most previous functional analyses of plant GSTFs have focused on tolerance to heavy metals, herbicides, drought, extreme temperatures, or salinity, but there is now evidence

to suggest that GSTFs are also involved in plant responses to biotic stresses (Sappl *et al.*, 2009; Gullner *et al.*, 2018). Plant GSTFs are generally induced by treatment with the defence-related plant hormone salicylic acid (Sappl *et al*., 2009; Gong *et al*. 2018), and it has been shown that some *AtGSTFs* are induced by fungal or bacterial pathogens (Sappl *et al.*, 2009). GSTF11 overexpression in oilseed rape (*Brassica napus*) increases resistance to the causal agent of powdery mildew, *Erysiphe cruciferarum* resulting in impaired mycelial growth (Mikhaylova *et al.*, 2021). Interestingly, GSTF9 has been implicated in the responses of cotton (*Gossypium arboretum*) and *A. thaliana* to the fungal pathogen *Verticillium dahliae* (Gong *et al.*, 2018). Cotton in which *GaGSTF9* is silenced and *Arabidopsis atgstf9* mutants have been shown to be more susceptible to *V. dahliae*, consistent with our finding for the interaction with *M. enterolobii*.

GSTFs are involved in anti-microbial metabolite synthesis and transport. AtGSTF6 has been implicated in the biosynthesis of the phytoalexin camalexin, whereas, AtGSTF2 is involved in the transport of defence-associated secondary metabolites such as camalexin and the flavonol quercetin-3-O-rhamnoside (Kumar, 2014). AtGSTF9, AtGSTF10 and AtGSTF11 have been shown to be involved in the biosynthesis of glucosinolates, a group of plant secondary metabolites with relevant nematicidal activity (Sonderby *et al.*, 2010; Eugui *et al*. 2022). We hypothesized that RKNs secrete MeMSP1 into the plant to highjack the functions of GSTFs to modulate host metabolism for their own benefit.

Combined analyses of transcriptomic and metabolomic analyses show that MeMSP1 modulates host metabolic pathways

We investigated the changes to plant responses induced by the effector through a combination of transcriptomics and metabolomics analysis. Such combined analyses have proved a powerful tool for deciphering plant responses to pathogens (Chen *et al.*, 2019; Duan *et al.*, 2022). Such analyses of the vascular tissues of *Eucalyptus urophylla* infected with *Ralstonia solanacearum* have revealed an activation of plant hormone signal transduction, flavonoid production, mitogen-activated protein kinase (MAPK) signalling, and amino-acid metabolism (Yang *et al.*, 2022). Many transcriptomic

studies have shown that most of the DEGs involved in the transcriptional reprogramming associated with the development of galls or giant cells are related to metabolism (Jammes *et al.*, 2005; Barcala *et al.*, 2010; Ji *et al.*, 2013; Portillo *et al.*, 2013). However, a few reports have focused on the changes in the host transcriptome induced by a single RKN effector (Shi *et al.*, 2018a and 2018b; Mejias *et al.*, 2021; Song *et al.*, 2021). A transcriptomic analysis of *A. thaliana* lines ectopically expressing MiMIF-2 and treated with flg22 revealed effects on metabolic pathways (Zhao *et al.*, 2020). We compared the transcriptomes and metabolomes of MeMSP1-OE *Arabidopsi*s lines with those of the WT. The DEGs and DAMs identified were enriched in metabolic pathways and secondary metabolite biosynthesis pathway.

We show here that primary metabolites, such as organic acids, amino acids and their derivatives, including GSH accumulate following the expression of a single effector in the plant, as previously reported in mature *Medicago truncatula* galls after RKN infection (Baldacci-Cresp *et al.*, 2012). GSH is involved in plant responses to pathogens, and, particularly, in the protection of plants against oxidized stress (Foyer & Noctor, 2009; Baldacci-Cresp *et al.*, 2012). Glutathione-deficient Arabidopsis mutants have an impaired activation of defence marker genes and of genes encoding proteins involved in the biosynthesis of the antimicrobial compound camalexin early in cyst nematode infection (Hasan *et al.*, 2022). Based on these findings, we hypothesise that the accumulation of GSH in MeMSP1-OE lines would help protect the giant cells from oxidative stress, enabling them to nourish the RKN successfully. The higher level of GSH in MeMSP1-OE lines at least partly accounts for their greater susceptibility to *M. enterolobii*. MeMSP1 expression affects plant metabolism, leading to the accumulation of primary metabolites. This may result in both the provision of more nutrients for nematode development and a decrease in the resources of the plant available for the production of defence compounds

MeMSP1 expression reduces the production of plant-defence related flavonoid compounds

Plants produce diverse secondary metabolites in response to infection with plant-

parasitic nematodes (Sato *et al*., 2019; Chen, *et al*., 2021). Certain metabolites may inhibit egg hatching or nematode motility, or even kill nematodes. Flavonoids are important members of this group of metabolites. Most of the metabolites downregulated in MeMSP1-OE lines are flavonoids. This group of specialised plant metabolites includes more than 10,000 different compounds. Plant GSTFs are involved in flavonoid biosynthesis (Shao *et al.*, 2021; Aktar *et al.*, 2022). Our understanding of the functions of almost all these substances remains poor, but there is increasing evidence to suggest a role for flavonoids in plant stress resistance (Sugiyama & Yazaki, 2014). There have been reports of flavonoid antimicrobial activity. For example, the maackiain produced by alfalfa and pea inhibits the growth of *Pythium graminicola* (Jiménez-González *et al.*, 2007) and *Rhizoctonia solani* (Guenoune *et al.*, 2001). Several flavonoids have recently been reported to have nematicidal activity, suggesting a possible role in plant-nematode interactions (Bano *et al.*, 2020). Various flavonols, including kaempferol and quercetin, have been shown to inhibit the chemotaxis and motility of nematodes (Wuyts *et al.*, 2006). Naringenin is a flavonoid that have been shown to have both antiviral and antifungal activity, including the inhibition of *Xanthomonas oryzae* growth and *Magnaporthe grisea* spore germination, and activity against *Fusarium* spp. (Den Hartogh & Tsiani, 2019). We show here that two flavonoids downregulated by MeMSP1, butin and naringenin, have lethal activity against *M. enterolobii*. This finding suggests that flavonoids play an important role in anti-nematode defences, and that nematodes may target their biosynthesis to promote parasitism.

This work sheds light on a novel effector mechanism targeting plant metabolism that decreases the production of plant defence-related compounds while favouring the accumulation of metabolites beneficial to the nematode, thereby promoting parasitism.

Acknowledgments

We thank Profs. Zejian Guo and Wenxian Sun, China Agricultural University, for their valuable suggestions. This research supported by the National Natural Science Foundation of China (no. 31772138), Sanya Yazhou Bay Science and Technology City

(SYND-2021-11), the National Key Research and Development Program of China (no. 2017YFD0200601). YC received scholarships from China Scholarship Council (nos. 201806350108) to study at INRA, France. PA, BF and MQ were supported by INRAE and by the French Government (National Research Agency, ANR) through the 'Investments for the Future' LabEx SIGNALIFE: programme reference#ANR-11-LABX-0028-01 and IDEX UCAJedi ANR-15-IDEX-0 and by the French-Chinese bilateral collaboration programme PHC XU GUANGQI (2020-2021).

Author contributions

YC designed, performed experiments and analysed the data. XS propagated the transgenic *Arabidopsis* lines. LL cloned the *MeMSP1* gene. SY and JZ constructed several vectors. YC and MQ analysed the RNA-seq data. QL and XW supervised some of this work and provided expertise. HJ, BF and PA were responsible for the development and management of the project. YC, PA, MQ, BF and HJ wrote the manuscript.

Competing interests

None declared.

Data availability

The data that support the findings of this study are available within the paper and within the supporting information of this article. The accession numbers of the genes mentioned in this study are shown in Accession numbers section of Materials and Methods. The transcriptome data are available at the Sequence Read Archive (SRA, https://www.ncbi.nlm.nih.gov/sra) via accession number PRJNA933796. The metabolomic data are available at MetaboLights (https://www.ebi.ac.uk/metabolights/) via accession number MTBLS7145.

References

Abad P, Gouzy J, Aury J, Castagnone-Sereno P, Danchin EGJ, Deleury E, Perfus-Barbeoch L, Anthouard V, Artiguenave F, Blok VC *et al.* 2008. Genome sequence of the metazoan plant-parasitic nematode *Meloidogyne incognita*. *Nature Biotechnology* **26**: 909-915.

Baldacci-Cresp F, Chang C, Maucourt M, Deborde C, Hopkins J, Lecomte P, Bernillon S, Brouquisse R, Moing A, Abad P *et al.* 2012. (Homo) glutathione deficiency impairs root-knot nematode development in *Medicago truncatula*. *PLoS Pathogens* **8**(1): e1002471.

Baldacci-Cresp F, Maucourt M, Deborde C, Pierre O, Moing A, Brouquisse R, Favery B, Frendo P. 2015. Maturation of nematode-induced galls in *Medicago truncatula* is related to water status and primary metabolism modifications. *Plant Science* **232**: 77-85.

Bano S, Iqbal EY, Lubna, Zik-ur-Rehman S, Fayyaz S, Faizi S. 2020. Nematicidal activity of flavonoids with structure activity relationship (SAR) studies against root knot nematode *Meloidogyne incognita*. *European Journal of Plant Pathology* **157**: 299-309.

Barcala M, Garcia A, Cabrera J, Casson S, Lindsey K, Favery B, Garcia-Casado G, Solano R, Fenoll C, Escobar C. 2010. Early transcriptomic events in microdissected *Arabidopsis* nematode-induced giant cells. *Plant Journal* **61**: 698-712.

Bartlem DG, Jones MG, Hammes UZ. 2014. Vascularization and nutrient delivery at root-knot nematode feeding sites in host roots. *Journal of Experimental Botany* **65**: 1789-1798.

Blok VC, Jones JT, Phillips MS, Trudgill DL. 2008. Parasitism genes and host range disparities in biotrophic nematodes: the conundrum of polyphagy versus specialisation. *Bioessays* **30**: 249-259.

Bybd DW, Kirkpatrick T, Barker KR. 1983. An improved technique for clearing and staining plant tissues for detection of nematodes. *Journal of Nematology* **15**:

142-143.

Caboni P, Ntalli NG, Aissani N, Cavoski I, Angioni A. 2012. Nematicidal activity of (e,e)-2,4-decadienal and (e)-2-decenal from *Ailanthus altissima* against *Meloidogyne javanica*. *Journal of Agricultural and Food Chemistry* **60**: 1146-1151.

Cabrera J, Bustos R, Favery B, Fenoll C, Escobar C. 2014. Nematic: a simple and versatile tool for the in silico analysis of plant-nematode interactions. *Molecular Plant Pathology* **15**: 627-636.

Castagnone-Sereno P. 2012. *Meloidogyne enterolobii* (= *M. mayaguensis*): profile of an emerging, highly pathogenic, root-knot nematode species. *Nematology* **14**: 133-138.

Chen C, Huang H, Wu CH. 2017. Protein bioinformatics databases and resources. *Methods Mol Biol* **1558**: 3-39.

Chen J, Lin B, Huang Q, Hu L, Zhuo K, Liao J. 2017. A novel *Meloidogyne graminicola* effector, MgGPP, is secreted into host cells and undergoes glycosylation in concert with proteolysis to suppress plant defenses and promote parasitism. *PLoS Pathogens* **13**: e1006301.

Chen L, Wu Q, He W, He T, Wu Q, Miao Y. 2019. Combined de novo transcriptome and metabolome analysis of common bean response to *Fusarium oxysporum* f. Sp. *phaseoli* infection. *International Journal of Molecular Sciences* **20**: 6278.

Chen W, Gong L, Guo Z, Wang W, Zhang H, Liu X, Yu S, Xiong L, Luo J. 2013. A novel integrated method for large-scale detection, identification, and quantification of widely targeted metabolites: application in the study of rice metabolomics. *Molecular Plant* **6**: 1769-1780.

Clough SJ, Bent AF. 1998. Floraldip: a simplified method for agrobacterium-mediated transformation of *Arabidopsis thaliana*. *Plant Journal* **16**: 9.

Dafny-Yelin M, Chung SM, Frankman EL, Tzfira T. 2007. pSAT RNA interference vectors: a modular series for multiple gene down-regulation in plants. *Plant Physiology* **145**: 1272-1281.

de Almeida EJ, Kyndt T, Vieira P, Van Cappelle E, Boudolf V, Sanchez V,

Escobar C, De Veylder L, Engler G, Abad P *et al.* 2012. Ccs52 and del1 genes are key components of the endocycle in nematode-induced feeding sites. *Plant Journal* **72**: 185-198.

Den Hartogh DJ, Tsiani E. 2019. Antidiabetic properties of naringenin: a citrus fruit polyphenol. *Biomolecules* **9**: 99.

Dixon DP, Hawkins T, Hussey PJ, Edwards R. 2009. Enzyme activities and subcellular localization of members of the *Arabidopsis* glutathione transferase superfamily. *Journal of Experimental Botany* **60**: 12.

Duan W, Peng L, Jiang J, Zhang H, Tong G. 2022. Combined transcriptome and metabolome analysis of strawberry fruits in response to powdery mildew infection. *Agronomy Journal* **114**: 1027-1039.

Eloh K, Sasanelli N, Maxia A, Caboni P. 2016. Untargeted metabolomics of tomato plants after root-knot nematode infestation. *Journal of Agricultural and Food Chemistry* **64**: 5963-5968.

Eugui D, Escobar C, Velasco P, Poveda J. 2022. Glucosinolates as an effective tool in plant-parasitic nematodes control: exploiting natural plant defenses. *Applied Soil Ecology* **176:** 104497.

Favery B, Dubreuil G, Chen M, Giron D, Abad P. 2020. Gall-inducing parasites: convergent and conserved strategies of plant manipulation by insects and nematodes. *Annual Review of Phytopathology* **58**: 1-22.

Foyer CH, Noctor G. 2009. Redox regulation in photosynthetic organisms: signaling, acclimation, and practical implications. *Antioxidants & Redox Signaling* **11**: 861-905.

Fraga CG, Clowers BH, Moore RJ, Zink EM. 2010. Signature-discovery approach for sample matching of a nerve-agent precursor using liquid chromatography-mass spectrometry, XCMS, and chemometrics. *Analytical Chemistry* **82**: 4165-4173.

Gong Q, Yang Z, Chen E, Sun G, He S, Butt HI, Zhang C, Zhang X, Yang Z, Du X, *et al.* 2018. A phi-class glutathione s-transferase gene for verticillium wilt resistance in *Gossypium arboreum* identified in a genome-wide association study. *Plant and Cell Physiology* **59**: 275-289.

Goverse A, Mitchum MG. 2022. At the molecular plant-nematode interface: new players and emerging paradigms. *Current Opinion in Plant Biology* **67**: 102225.

Guenoune D, Galili S, Phillips DA, Volpin H, Chet I, Okon Y, Kapulnik Y. 2001. The defense response elicited by the pathogen *Rhizoctonia solani* is suppressed by colonization of the AM-fungus glomus intraradices. *Plant Science* **160**: 925-932.

Gullner G, Komives T, Kiraly L, Schroder P. 2018. Glutathione s-transferase enzymes in plant-pathogen interactions. *Frontiers in Plant Science* **9**:1836.

Guo, B., Lin, B., Huang, Q., Li, Z., Zhuo, K. & Liao, J. (2022) A nematode effector inhibits plant immunity by preventing cytosolic free Ca^{2+} rise. *Plant, Cell & Environment* **45:** 3070-3085.

Haegeman A, Mantelin S, Jones JT, Gheysen G. 2012. Functional roles of effectors of plant-parasitic nematodes. *Gene* **492**: 19-31.

Hasan MS, Chopra D, Damm A, Koprivova A, Kopriva S, Meyer AJ, Mueller-Schuessele S, Grundler FMW, Siddique S. 2022. Glutathione contributes to plant defence against parasitic cyst nematodes. *Molecular Plant Pathology* **23**: 1048-1059.

Horváth E, Bela K, Papdi C, Gallé Á, Szabados L, Tari I, Csiszár J. 2015. The role of Arabidopsis glutathione transferase F9 gene under oxidative stress in seedlings. *Acta Biologica Hungarica* **66**: 406-418.

Huang G, Gao B, Maier T, Allen R, Davis EL, Baum TJ, Hussey RS. 2003. A profile of putative parasitism genes expressed in the esophageal gland cells of the root-knot nematode *Meloidogyne incognita*. *Molecular Plant-Microbe Interactions* **16**: 376-381.

Jagdale S, Rao U, Giri AP. 2021. Effectors of root-knot nematodes: an arsenal for successful parasitism. *Frontiers in Plant Science* **12**: 800030.

Jammes F, Lecomte P, de Almeida-Engler J, Bitton F, Martin-Magniette ML, Renou JP, Abad P, Favery B. 2005. Genome-wide expression profiling of the host response to root-knot nematode infection in Arabidopsis. *Plant Journal* **44**: 447-458.

Ji H, Gheysen G, Denil S, Lindsey K, Topping JF, Nahar K, Haegeman A, De Vos WH, Trooskens G, Van Criekinge W *et al.* 2013. Transcriptional analysis through RNA sequencing of giant cells induced by *Meloidogyne graminicola* in rice

780 roots. *Journal of Experimental Botany* **64**: 3885-3898.
781 **Jiménez-González L, Álvarez-Corral M, Muñoz-Dorado M, Rodríguez-García I.**
782 **2007.** Pterocarpans: interesting natural products with antifungal activity and other
783 biological properties. *Phytochemistry Reviews* **7**: 125-154.
784 **Ji-xiang C, Bao-an S. 2021.** Natural nematicidal active compounds: recent research
785 progress and outlook. *Journal of Integrative Agriculture* **20**: 2015-2031.
786 **Jones JT, Haegeman A, Danchin EG, Gaur HS, Helder J, Jones MG, Kikuchi T,**
787 **Manzanilla-Lopez R, Palomares-Rius JE, Wesemael WM *et al.* 2013.** Top 10
788 plant-parasitic nematodes in molecular plant pathology. *Molecular Plant Pathology*
789 **14**: 946-961.
790 **Kumar D. 2014.** Salicylic acid signaling in disease resistance. *Plant Science* **228**:
791 127-134.
792 **Langmead B, Trapnell C, Pop M, Salzberg SL. 2009.** Ultrafast and memory-
793 efficient alignment of short DNA sequences to the human genome. *Genome Biology*
794 **10**: R25.
795 **Li B, Dewey CN. 2011.** RSEM: accurate transcript quantification from RNA-seq data
796 with or without a reference genome. *BMC Bioinformatics* **12**: 323.
797 **Li X, Yang D, Niu J, Zhao J, Jian H. 2016.** De novo analysis of the transcriptome
798 of *Meloidogyne enterolobii* to uncover potential target genes for biological control.
799 *International Journal of Molecular Sciences* **17:** 14429.
800 **Love MI, Huber W, Anders S. 2014.** Moderated estimation of fold change and
801 dispersion for RNA-seq data with deseq2. *Genome Biology* **15**: 550.
802 **Mejias J, Bazin J, Truong NM, Chen Y, Marteu N, Bouteiller N, Sawa S, Crespi**
803 **MD, Vaucheret H, Abad P et al.. 2021.** The root-knot nematode effector MiEFF18
804 interacts with the plant core spliceosomal protein smd1 required for giant cell
805 formation. *The New Phytologist* **229**: 3408-3423.
806 **Mejias J, Chen Y, Bazin J, Truong N, Mulet K, Noureddine Y, Jaubert-Possamai**
807 **S, Ranty-Roby S, Soulé S, Abad P *et al.* 2022.** Silencing the conserved small
808 nuclear ribonucleoprotein smd1 target gene alters susceptibility to root-knot
809 nematodes in plants. *Plant Physiology* **189**: 1741-1756.

Mejias J, Truong NM, Abad P, Favery B, Quentin M. 2019. Plant proteins and processes targeted by parasitic nematode effectors. *Frontiers in Plant Science* **10**: 970.

Mikhaylova E, Khusnutdinov E, Shein MY, Alekseev VY, Nikonorov Y, Kuluev B. 2021. The role of the gstf11 gene in resistance to powdery mildew infection and cold stress. *Plants* **10**: 2729.

Mitchum MG, Hussey RS, Baum TJ, Wang X, Elling AA, Wubben M, Davis EL. 2013. Nematode effector proteins: an emerging paradigm of parasitism. *The New Phytologist* **199**: 879-894.

Niu J, Liu P, Liu Q, Chen C, Guo Q, JunmeiYin, GuangsuiYang, Jian H. 2016. Msp40 effector of root-knot nematode manipulates plant immunity to facilitate parasitism. *Scientific Reports* **6:** 19443.

Oakley A. 2011. Glutathione transferases: a structural perspective. *Drug Metabolism Reviews* **43**: 138-151.

Philbrick AN, Adhikari TB, Louws FJ, Gorny AM. 2020. *Meloidogyne enterolobii*, a major threat to tomato production: current status and future prospects for its management. *Frontiers in Plant Science* **11**: 606395.

Portillo M, Cabrera J, Lindsey K, Topping J, Andres MF, Emiliozzi M, Oliveros JC, Garcia-Casado G, Solano R, Koltai H *et al.* 2013. Distinct and conserved transcriptomic changes during nematode-induced giant cell development in tomato compared with Arabidopsis: a functional role for gene repression. *The New Phytologist* **197**: 1276-1290.

Rocha M, Bournaud C, Dazeniere J, Thorpe P, Bailly-Bechet M, Pellegrin C, Pere A, Grynberg P, Perfus-Barbeoch L Eves-van den Akker et al. 2021. Genome expression dynamics reveal the parasitism regulatory landscape of the root-knot nematode *Meloidogyne incognita* and a promoter motif associated with effector genes. *Genes* **12**: 771.

Rutter WB, Franco J, Gleason C. 2022. Rooting out the mechanisms of root-knot nematode-plant interactions. *Annual Review of Phytopathology* **60**: 43-76.

Sappl PG, Carroll AJ, Clifton R, Lister R, Whelan J, Harvey MA, Singh KB.

2009. The Arabidopsis glutathione transferase gene family displays complex stress regulation and co-silencing multiple genes results in altered metabolic sensitivity to oxidative stress. *Plant Journal* **58**: 53-68.

Sato K, Kadota Y, Shirasu K. 2019. Plant immune responses to parasitic nematodes. *Frontiers in Plant Science* **10**: 1165.

Shi Q, Mao Z, Zhang X, Ling J, Lin R, Zhang X, Liu R, Wang Y, Yang Y, Cheng X, Xie B. 2018a. The novel secreted *Meloidogyne incognita* effector miise6 targets the host nucleus and facilitates parasitism in *Arabidopsis*. *Frontiers in Plant Science* **9**: 252.

Shi Q, Mao Z, Zhang X, Zhang X, Wang Y, Ling J, Lin R, Li D, Kang X, Sun W, Xie B. 2018b. A *Meloidogyne incognita* effector *MiISE5* suppresses programmed cell death to promote parasitism in host plant. *Scientific Reports* **8**: 7256.

Sikandar A, Jia L, Wu H, Yang S. 2022. *Meloidogyne enterolobii* risk to agriculture, its present status and future prospective for management. *Frontiers in Plant Science* **13**: 1093657.

Sonderby IE, Geu-Flores F, Halkier BA. 2010. Biosynthesis of glucosinolates--gene discovery and beyond. *Trends in Plant Science* **15**: 283-290.

Song H, Lin B, Huang Q, Sun L, Chen J, Hu L, Zhuo K, Liao J. 2021. The *Meloidogyne graminicola* effector MgMO289 targets a novel copper metallochaperone to suppress immunity in rice. *Journal of Experimental Botany* **72**: 5638–5655.

Su T, Xu J, Li Y, Lei L, Zhao L, Yang H, Feng J, Liu G, Ren D. 2011. Glutathione-indole-3-acetonitrile is required for camalexin biosynthesis in *Arabidopsis thaliana*. *The Plant Cell* **23**: 364-380.

Sugiyama A, Yazaki K. 2014. Flavonoids in plant rhizospheres: secretion, fate and their effects on biological communication. *Plant Biotechnology* **31**: 431-443.

Tian T, Liu Y, Yan H, You Q, Yi X, Du Z, Xu W, Su Z. 2017. Agrigo v2.0: a go analysis toolkit for the agricultural community, 2017 update. *Nucleic Acids Research* **45**: W122-W129.

Varet H, Brillet-Gueguen L, Coppee JY, Dillies MA. 2016. SARtools: a DESeq2- and EdgeR-based R pipeline for comprehensive differential analysis of rna-seq data. *PLoS One* **11**(6): e157022.

Verma A, Lee C, Morriss S, Odu F, Kenning C, Rizzo N, Spollen WG, Lin M, McRae AG, Givan SA, Hewezi T, Hussey R, Davis EL, Baum TJ, Mitchum MG. 2018. The novel cyst nematode effector protein 30d08 targets host nuclear functions to alter gene expression in feeding sites. *The New Phytologist* **219**: 697-713.

Vieira P, Danchin EGJ, Neveu C, Crozat C, Jaubert S, Hussey RS, Engler G, Abad P, de Almeida-Engler J, Castagnone-Sereno P, Rosso M. 2011. The plant apoplasm is an important recipient compartment for nematode secreted proteins. *Journal of Experimental Botany* **62**: 1241-1253.

Walter M, Chaban C, Schutze K, Batistic O, Weckermann K, Nake C, Blazevic D, Grefen C, Schumacher K, Oecking C, Harter K, Kudla J. 2004. Visualization of protein interactions in living plant cells using bimolecular fluorescence complementation. *Plant Journal* **40**: 428-438.

Wuyts N, Swennen R, De Waele D. 2006. Effects of plant phenylpropanoid pathway products and selected terpenoids and alkaloids on the behaviour of the plant-parasitic nematodes *Radopholus similis*, *Pratylenchus penetrans* and *Meloidogyne incognita*. *Nematology* **8**: 89-101.

Xie C, Mao X, Huang J, Ding Y, Wu J, Dong S, Kong L, Gao G, Li CY, Wei L. 2011. Kobas 2.0: a web server for annotation and identification of enriched pathways and diseases. *Nucleic Acids Research* **39**: W316-W322.

Yamaguchi YL, Suzuki R, Cabrera J, Nakagami S, Sagara T, Ejima C, Sano R, Aoki Y, Olmo R, Kurata T, Obayashi T, Demura T, Ishida T, Escobar C, Sawa S. 2017. Root-knot and cyst nematodes activate procambium-associated genes in Arabidopsis roots. *Frontiers in Plant Science* **8**: 1195.

Yang B, Eisenback JD. 1983. *Meloidogyne enterolobii* n. Sp. (Meloidogynidae), a root-knot nematode parasitizing pacara earpod tree in China. *Journal of Nematology* **15**: 381-391.

Yang XH, Huang J, Yang HX, Liao HQ, Xu F, Zhu BZ, Xu XY, Zhang L, Huang

HY, Du QZ, Pan W. 2022. Transcriptome and metabolome profiling in different stages of infestation of *Eucalyptus urophylla* clones by *Ralstonia solanacearum*. *Molecular Genetics and Genomics* **297**: 1081-1100.

Zhang S, Ying H, Pingcuo G, Wang S, Zhao F, Cui Y, Shi J, Zeng H, Zeng X. 2019. Identification of potential metabolites mediating bird's selective feeding on *Prunus mira* flowers. *Biomedical Research International* **2019**: 1395480.

Zhao J, Li L, Liu Q, Liu P, Li S, Yang D, Chen Y, Pagnotta S, Favery B, Abad P, Jian H. 2019. A mif-like effector suppresses plant immunity and facilitates nematode parasitism by interacting with plant annexins. *Journal of Experimental Botany* **70**: 5943-5958.

Zhao J, Mao Z, Sun Q, Liu Q, Jian H, Xie B. 2020. MiMIF-2 effector of *Meloidogyne incognita* exhibited enzyme activities and potential roles in plant salicylic acid synthesis. *International Journal of Molecular Sciences* **21**: 3507.

Zhao J, Mejias J, Quentin M, Chen Y, de Almeida-Engler J, Mao Z, Sun Q, Liu Q, Xie B, Abad P, Favery B, Jian H. 2020. The root-knot nematode effector mipdi1 targets a stress-associated protein, SAP, to establish disease in Solanaceae and Arabidopsis. *The New Phytologist* **228**:1417–1430.

Zhao J, Sun Q, Quentin M, Ling J, Abad P, Zhang X, Li Y, Yang Y, Favery B, Mao Z, Xie B. 2021. A *Meloidogyne incognita* c-type lectin effector targets plant catalases to promote parasitism. *The New Phytologist* **232**: 2124-2137.

Zhuo K, Chen J, Lin B, Wang J, Sun F, Hu L, Jinling Liao A. 2017. A novel *Meloidogyne enterolobii* effector metctp promotes parasitism by suppressing programmed cell death in host plants. *Molecular Plant pathology* **18**: 45-54.

Supporting Information

Additional Supporting Information may be found online in the Supporting Information section at the end of the article.

Fig. S1 *MeMSP1* is a putative dorsal gland effector gene containing the Mel-DOG motif.

Fig. S2 Both *MeMSP1* and *MiMSP1* are upregulated in the parasitic stage of root-knot nematodes.

Fig. S3 Western blot analysis verified specificity of MeMSP1 antibodies.

Fig. S4 Localisation of MeMSP1 in parasitic stages of *M. enterolobii*.

Fig. S5 Localisation of MeMSP1 in tomato root gall sections of *M. enterolobii*.

Fig. S6 *In planta* RNA interference (RNAi) and ectopic expression of MeMSP1 in *Arabidopsis* shows MeMSP1 participated in the parasitism of *M. enterolobii*.

Fig. S7 Verification of the MeMSP1 expression in *MeMSP1* overexpressing *Arabidopsis* lines by western blot.

Fig. S8 eGFP fused MeMSP1 localised in the cytosol of *Nicotiana benthamiana* epidermal leaf cells.

Fig. S9 Bimolecular fluorescent complementation (BiFC) shows that MeMSP1 interact with all the members of AtGSTFs, but not with the negative controls (AtGSTU19 and empty vector).

Fig. S10 Alignment of AtGSTF9 and its mutant protein sequences.

Fig. S11 Verification of homozygous T-DNA insertion mutants of the *Arabidopsis AtGSTF9*.

Fig. S12 The *Arabidopsis gstf9* mutant is more susceptible to *M. enterolobii* than the WT.

Fig. S13 Validation of eight differentially expressed genes (DEGs) identified in the MeMSP1-OE *Arabidopsis* lines through RT-qPCR.

Fig. S14 The expression of *MeMSP1* affects the oxidation-reduction balance in *Arabidopsis*.

Fig. S15 Three of five down-regulated metabolites shows a paralysis effect on nematodes**.**

Fig. S16 Down-regulated metabolites butin and naringenin in MeMSP1-OE *Arabidopsis* lines shows a paralysis effect on nematodes.

Table S1 Primers used in this study.

Table S2 Potential targets of MeMSP1 in *Arabidopsis* identified by immunoprecipitation (IP) followed by liquid chromatography-tandem mass spectrometry (LC-MS) in both MeMSP-OE lines and not in control WT line.

Table S3 Expression of AtGSTFs in giant cells and galls induced by root-knot nematodes.

Table S4 Differentially expressed genes (DEGs) in MeMSP1-OE-1 *Arabidopsis* line.

Table S5 Differentially expressed genes (DEGs) in MeMSP1-OE-3 *Arabidopsis* line.

Table S6 Differentially expressed genes (DEGs) in both MeMSP1-OE *Arabidopsis* lines and their expression pattern in root-knot nematode-infected tissues

Table S7 Differently accumulated metabolites (DAMs) in MeMSP1-OE-1 *Arabidopsis* line.

Table S8 Differently accumulated metabolites (DAMs) in MeMSP1-OE-3 *Arabidopsis* line.

Table S9 Amino acids detected in MeMSP1-OE *Arabidopsis* lines.

Figure legends

Table 1 Differentially accumulated metabolites shared by MeMSP1-OE-1 and MeMSP1-OE-3 *Arabidopsis* lines

Class	Compounds	LogFC(MeMSP1-OE-1)	LogFC(MeMSP1-OE-3)	Type
Amino acid derivatives	3-Chloro-L-tyrosine	1.13	1.01	up
	Glutathione reduced form (GSH)	1.49	3.00	up
	S-(methyl)glutathione	1.42	1.61	up
	γ-Glu-Cys	1.55	2.60	up
	CYS-GLY	2.53	3.26	up
	L-Alanine	1.67	1.31	up
Nucleotide and its derivates	N-Methylnicotinamide	-1.35	-1.43	down
	Adenosine 3'-monophosphate	2.71	1.49	up
	Inosine 5'-monophosphate	2.18	1.47	up
	Adenosine 5'-monophosphate	1.95	1.07	up
Organic acids	Argininosuccinate	1.37	1.72	up
	Diethyl phosphate	1.72	1.40	up
Quinate and its derivatives	O-Sinapoyl quinic acid	1.65	1.31	up
Tryptamine derivatives	N-Feruloyl serotonin	2.15	1.06	up
	6-Hydroxymelatonin	-1.23	-2.47	down
Vitamins	Pyridoxal 5'-phosphate	1.47	1.88	up
Hydroxycinnamoyl derivatives	1-O-beta-D-Glucopyranosyl sinapate	1.44	1.11	up
Lipids_Glycerophospholipids	LysoPC 16:2	1.23	2.25	up
Others	O-Phosphorylethanolamine	1.11	1.29	up
Anthocyanins	Pelargonin	2.11	1.44	up
Proanthocyanidins	Procyanidin A3	1.34	1.13	up
Catechin derivatives	(+)-Gallocatechin (GC)	1.25	1.14	up
Coumarins	N-sinapoyl hydroxycoumarin	1.35	1.26	up
	O-Feruloyl 4-hydroxylcoumarin	1.44	1.60	up
Flavanone	Naringenin	-2.10	-3.90	down
	Naringenin chalcone	-15.85	-15.85	down
Flavone	Chrysoeriol O-rhamnosyl-O-glucuronic acid	-2.34	-4.11	down
	Acacetin	15.16	15.52	up
	Butin	-15.80	-15.80	down
Flavone C-glycosides	Chrysin C-hexoside	-2.29	-2.31	down
	di-C,C-hexosyl-apigenin	-2.22	-2.33	down
	8-C-hexosyl-luteolin O-hexoside	-1.59	-1.15	down
Flavonol	Quercetin 3-alpha-L-arabinofuranoside (Avicularin)	2.30	2.65	up
Flavonolignan	Tricin 4'-O-(β-guaiacylglyceryl) ether O-hexoside	-2.72	-2.36	down
	Tricin 4'-O-syringyl alcohol	-1.29	-11.44	down
Phenolamides	N', N''-di-p-coumaroyl spermidine	-14.85	-14.85	down
	N-sinapoyl cadaverine	-1.23	-14.31	down
	N-Sinapoyl agmatine	1.46	1.34	up
Magenta background	Significantly upregulated accumulation			
Green background	Significantly downregulated accumulation			

976

Fig. 1 *MSP1* is a conserved effector in root-knot nematodes. (a) Alignment of MeSP1-like proteins from different *Meloidogyne* species using ClustalW2. Identical amino acids residues are highlighted against black background shading, highly similar (>75%) amino acid residues are shown in pink background shading. (b) Maximum likelihood phylogenetic tree of MSP1 sequences. Numbers at tree nodes represent bootstrap support values. Support for the nodes was calculated with a hundred bootstrap replicates. MiMSP12 was used as outgroup.

Fig. 2 MeMSP1 is a dorsal gland protein secreted in the giant cells. (a) Localisation of MeMSP1 in the dorsal glands of *M. enterolobii* preparasitic J2s through *in situ* hybridisation. Fixed J2s were hybridised with antisense cDNA probes from MeMSP1 (Figure S1). (b) No signal has been observed when the sense probe was used as a negative control. (c-e) Immunolocalisation on parasitic nematodes extracted from infected root at 14 dpi. The use of anti-MeMSP1 antibodies showed the specific production of MeMSP1 in the dorsal gland of parasitic nematodes (c) and its delivery in the oesophagus (d) of parasitic nematodes. No signal was observed when pre-immune serum was used as a negative control (e). (f-i) Immunolocalisation in sectioned tomato root galls at 14 dpi. Secreted MeMSP1 protein signal were detected in the cytoplasm of the giant cells (f, g, h). No signal was observed when pre-immune serum was used as a negative control (i). Micrographs (c-e) are overlay of images of the bright and Alexa Fluor 488 fluorescence. Micrographs (f-i) are merge of images of the Alexa Fluor 488-conjugated secondary antibodies, DAPI-stained nuclei and differential interference contrast. N, nematode; Asterisks *, giant cells; Red arrow, signals of Alexa Fluor 488 fluorescence; M, metacorpus. The dashed white line marks the outline of a giant cell. Scale bars: (a and, b) 20 μm, (c, d, e and i) 100 μm, (f and h) 75 μm or (g) 50 μm.

Fig. 3 *In planta* RNA interference (RNAi) and ectopic expression of *MeMSP1* in *Arabidopsis* shows MeMSP1 participated in the parasitism of *M. enterolobii*. (a) The relative expression level of *MeMSP1* in *M. enterolobii* collected from three

independent, homozygous *MeMSP1-RNAi* lines (MeMSP1-Ri-1, -2 and -3), *GFP-RNAi* line (GFP-Ri) and wild type (COL) Arabidopsis. Error bars represent +/- SD. (b) *In planta* RNAi of *MeMSP1* reduced *M. enterolobii* infection. Galls, nematodes (all stages *in planta*) and adult females (n=15) were counted at 30 dpi. The experiments were performed three times with similar results. (c) *MeMSP1* overexpression in Arabidopsis increased susceptibility to *M. enterolobii*. Galls, nematodes (all stages *in planta*) and adult females (n=15) were counted at 30 dpi in two independent, homozygous *MeMSP1* overexpressing lines (MeMSP1-OE-1 and -3), empty vector control line (super1300) and wild type (COL) Arabidopsis. The experiments were performed three times with similar results and the results of the other two tests were shown in Fig. S6. (b, c, d) Boxes indicate interquartile range (25–75th percentile). The central lines within the boxes represent medians. Whiskers represent extreme values that are not outliers. The "+" in the boxes represent average values. The black dots outside the box represents outliers. Different letters indicate statistically significant difference in one-way ANOVA with Dunnett's multiple comparisons test ($P<0.05$).

Fig. 4 MeMSP1 interacts with all the AtGSTF members from Arabidopsis *in vivo* and *in planta*. (a) Co-immunoprecipitation was used to verify the interaction between AtGSTF family members and MeMSP1. WB (western blotting) assay confirmed expressions of input proteins: Flag-AtGSTFs, Flag-GFP (anti-Flag antibodies) and MeMSP-HA (anti-HA antibodies). In the samples after immunoprecipitation, MeMSP1-HA was detected when co-expressing with Flag -AtGSTFs, but not when co-expressing with Flag-GFP. (b) Bimolecular fluorescence complementation (BiFC) visualization of the interaction between some AtGSTFs and MeMSP1. Images were obtained 48 h after co-infiltration in *N. benthamiana* leaves. YFP, yellow fluorescent protein. Scale bar, 100 μm. BIFC images of the interaction between MeMSP1 and all the members of AtGSTF were provided in supplement Fig. S9.

Fig. 5 The N-terminal of AtGSTF9 is essential to their interaction and AtGSTF9 has a role in plant immunity to nematodes. (a) BiFC visualization of the interactions between

the mutated AtGSTF9 and MeMSP1. The corresponding proteins were co-expressed in tobacco leaves. Images were obtained 48 h after co-expression. Scale bar, 100 μm. (b) The *Arabidopsis gstf9* mutants are more susceptible to *M. enterolobii* than the WT. Galls and nematodes (n≥22) were counted at 30 dpi. The experiments were performed two times with similar results and the result of the other test was shown in Fig. S10. Boxes indicate interquartile range (25–75th percentile). The central lines within the boxes represent medians. Whiskers represent extreme values that are not outliers. The "+" in the boxes represent average values. Different letters indicate statistically significant difference in one-way ANOVA with Dunnett's multiple comparisons test ($P<0.05$).

Fig. 6 MeMSP1 affects the expression of metabolic-related genes in *Arabidopsis*. (a, b) Venn diagram showing overlap between two MeMSP1 transgenic lines differentially expressed genes compared to Col-0. (c) KEGG classification of differentially expressed genes shared by two MeMSP1 transgenic lines. The ordinate represents the KEGG pathway, and the abscissa represents number of genes.

Fig. 7 MeMSP1 affect the metabolic pathway and biosynthesis of secondary metabolites pathway in *Arabidopsis*. (a, b) Venn diagram showing overlap between two MeMSP1 transgenic lines differentially expressed metabolites compared to Col-0. (c) KEGG classification of differentially expressed metabolites shared by two MeMSP1 transgenic lines. The ordinate represents the KEGG pathway, and the abscissa represents number of metabolites.

Fig. 8 Down-regulated metabolites butin and naringenin in MeMSP1-OE *Arabidopsis* lines shows a paralysis effect on nematodes. (a) Butin and naringenin show a paralysis effect on nematodes at different concentration and time. CK, control check which consisted of the corresponding concentration of DMSO. Boxes indicate interquartile range (25–75th percentile). The central lines within the boxes represent medians. Whiskers represent extreme values that are not outliers. The "+" in the boxes represent

average values. * indicate statistically significant difference in one-way ANOVA with Dunnett's multiple comparisons test ($P<0.05$). The experiments were performed three times with similar results and the results of the other two tests were shown in Fig. S16. (b) The nematodes pictures from CK treatment at 48 h. (c) Picture of nematode treated with 50μg/ml butin for 48 hours. (d) Picture of nematodes treated with 50μg/ml naringenin for 48 hours. (c, d) Red arrow, paralysed/dead nematode. Scale bars: (b, c, d) 1000 μm.

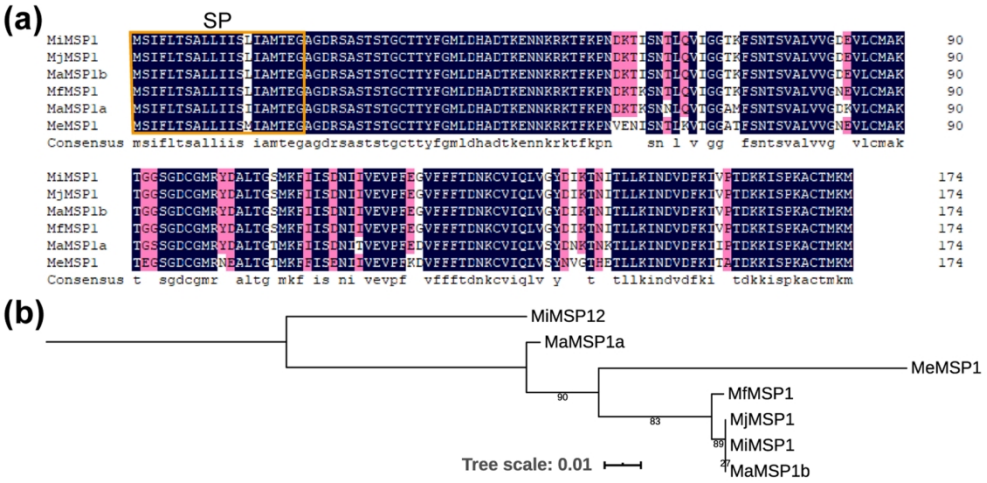

Fig 1

160x80mm (300 x 300 DPI)

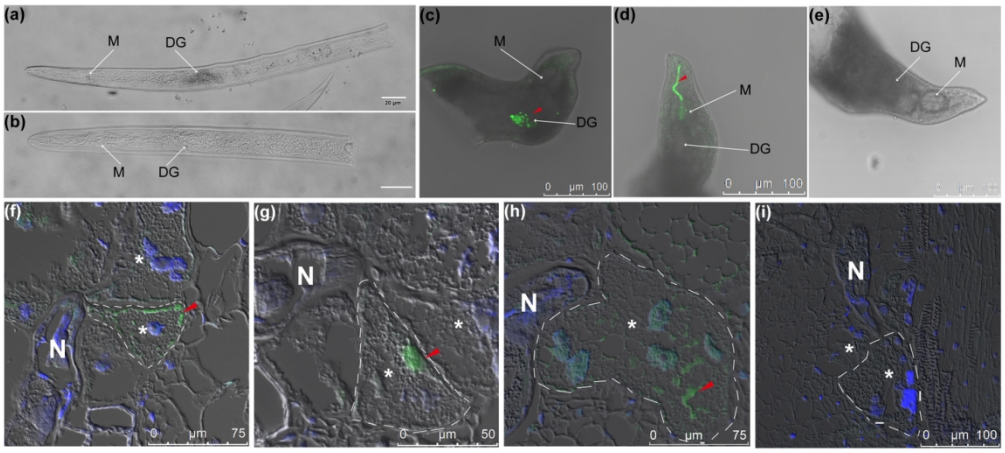

Fig 2_new_R3

123x55mm (300 x 300 DPI)

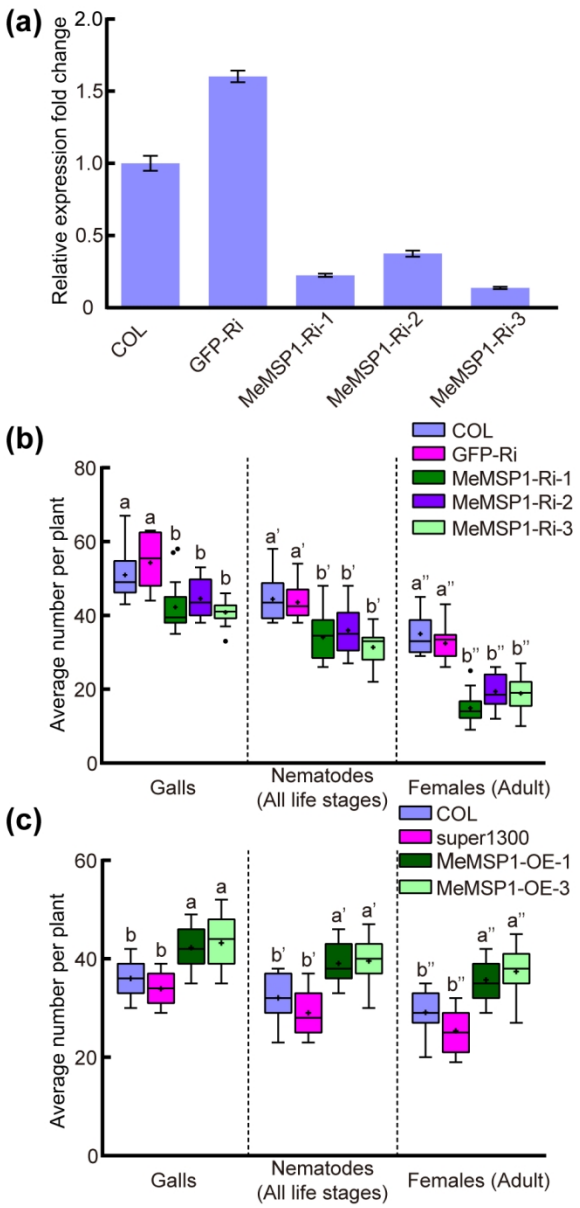

Fig 3

80x166mm (300 x 300 DPI)

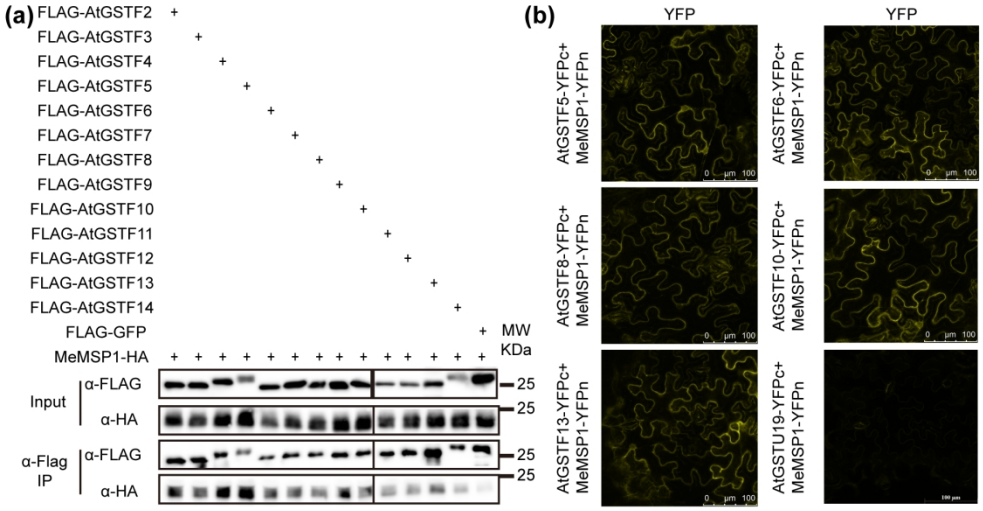

Fig 4

174x91mm (300 x 300 DPI)

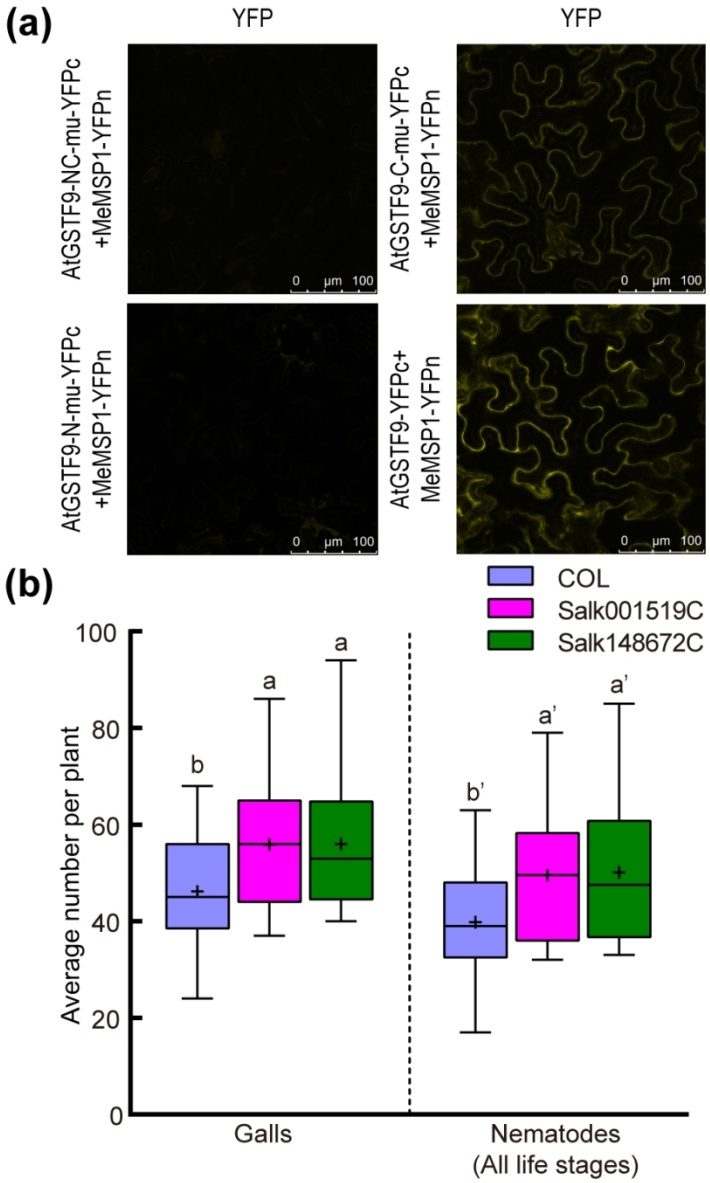

Fig 5

80x131mm (300 x 300 DPI)

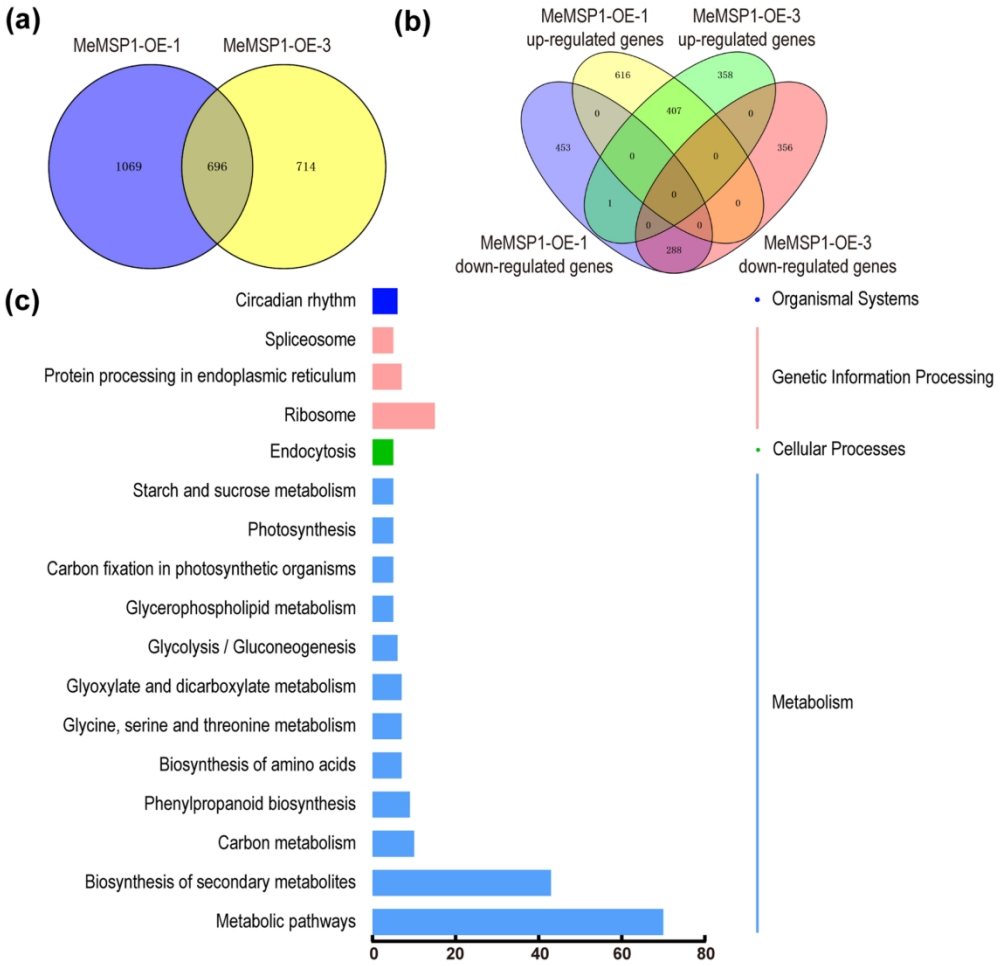

Fig 6

160x157mm (300 x 300 DPI)

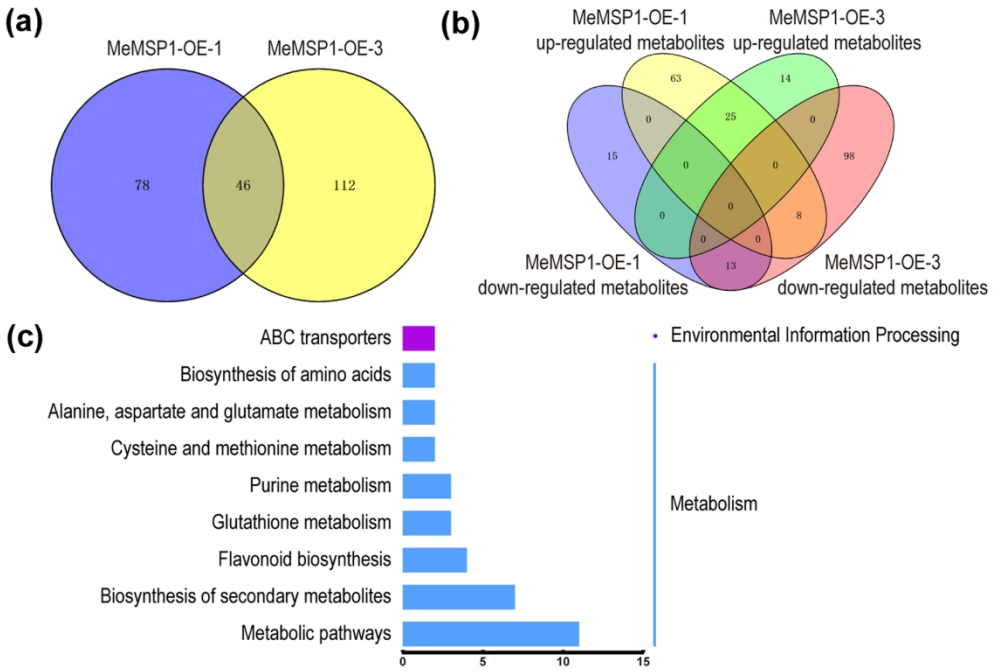

Fig 7

160x108mm (300 x 300 DPI)

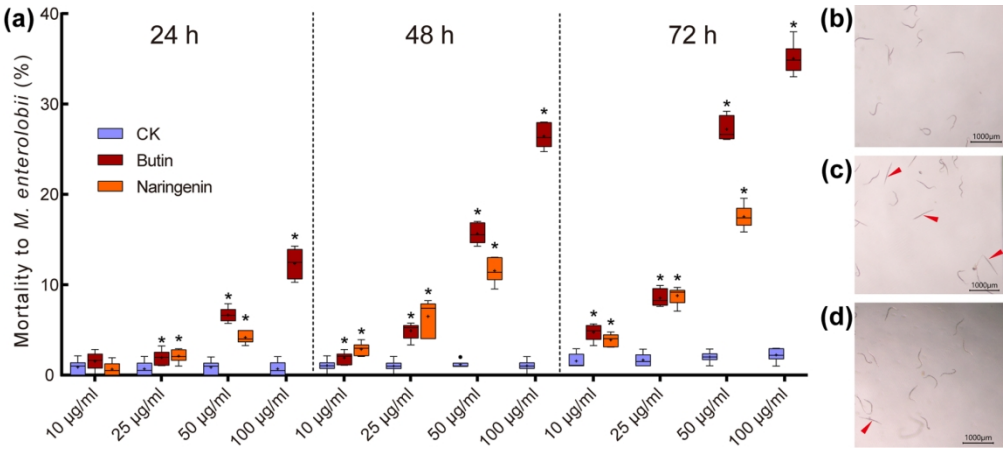

Fig 8

160x70mm (300 x 300 DPI)